Structural, Energetic, and Spectroscopic Features of Lower Energy Complexes of Superoxide Hydrates $O_2^-(H_2O)_{1-4}$

Victor Ya. Antonchenko[†] and Eugene S. Kryachko*[,†,§]

Bogoliubov Institute for Theoretical Physics, Kiev, 03143 Ukraine, and Department of Chemistry, Bat. B6C, University of Liege, Sart-Tilman, B-4000 Liege, Belgium

Received: August 4, 2004; In Final Form: February 4, 2005

The lower-energy portions of the potential energy surfaces of superoxide hydrates $O_2^-(H_2O)_{1\le n\le 4}$ are thoroughly investigated at high computational levels. The structural, energetic and spectroscopic features of the stable superoxide hydrates on these potential energy surfaces are discussed, focusing in particular on some implications to their infrared spectra and the hydrogen bond trends. The present work reports the transition-state linkers between the most stable superoxide hydrates which are useful to understand the energetics of their mutual interconversions.

1. Introduction

The superoxide radical $O_2^{-\bullet}$ is one of the most ubiquitous and continuous byproducts of respiration that is also generated in mammalian cells during the inflammatory response and has been implicated in the etiology and/or progression of a variety of pathophysiologies ranging from cancer to rheumatoid arthritis, diabetes, cardiovascular diseases, atherosclerosis, essential hypertension, Alzheimer's disease, and aging, too.[1,2] Reacting with the side chains of lysine, arginine, proline, threonine, and glutamic acid residues, superoxide forms carbonyl derivatives.[1h,j,2i] Its reaction with protein backbone causes a cleavage of the peptide main chain.[1h,2i] Superoxide is known as "a molecular loose cannon"[1g] that oxidizes molecules in the cell and causes mutations in DNA and damage in proteins.[2h,i] Enzymes convert superoxide to hydrogen peroxyde by means of a so-called superoxide dismutases.[1f,2f−h]

Superoxide is always formed via a solar irradiation of some materials dissolved in rivers and oceans. Near a surface of water, a so-called sunlit region, dissolved organic materials undergo photochemical reactions with oxygen particularly yielding, at relatively high rates, superoxide having a rather large lifetime. For example, its steady-state concentration may reach 10^{-8}−10^{-7} mol/L and its lifetime becomes of the order of many minutes.

As a major anionic charge carrier, superoxide is present in the atmosphere where it is clustered with abundant atmospheric species such as water and carbon dioxide.[3] Interacting with water, it forms hydrated superoxide clusters $O_2^-(H_2O)_n$[4] which have been of considerable interest for several reasons. One of them, purely theoretical, arises from the theory of intermolecular interaction in a sense of what is a preferential interaction in hydrated superoxide: the anion−water interaction or the water−water hydrogen bonding? As would be anticipated, the former is mostly responsible for a building of a first hydration shell ($n = 1-4$?) around O_2^- that screens the negative charge, localized on the oxygen molecule, via bonding water molecules to the lobes of the antibonding π^* singly occupied molecular orbital (SOMO) of superoxide. The latter seems to play a major role in the outer hydration shells.

It, however, appears that the structures of the $O_2^-(H_2O)_n$, in particular for $n = 1$, have been debated during nearly the two past decades.[4−7] A varience has appeared in whether the most stable monohydrated superoxide species adopt a symmetric C_{2v} structure with a water molecule as a double-proton donor or an asymmetric one with a lower symmetry C_s possessing a single hydrogen-bonded bridge between a water molecule and the superoxide? The recent study by Robinson et al.,[6d] based on using the quadratic configuration interaction QCISD(T) method in conjunction with 6-31+G(d,p), 6-31++G(d,p), and 6-311+G-(d,p) basis sets, has likely resolved this paradigm and definitely placed the C_s structure at the global minimum and the C_{2v} as the transition state lying higher by ∼0.9 kcal/mol (QCISD(T)/6-311++G(d,p)//QCISD/6-311++G(d,p)). Nevertheless, the new cluster spectroscopy experiments[7] on $O_2^-(H_2O)_n$ ($n = 1-4$) have revealed a rather diffuse infrared spectra of $O_2^-(H_2O)_{1-3}$ clusters that frustrate a definitive identification of their structures, in contrast to the superoxide tetrahydrate whose structure, as believed, can be well determined from the infrared spectra and has recently been obtained at the B3LYP/6-311+G(2d,p) computational level.[7a] Diffuse infrared patterns for $O_2^-(H_2O)_{1-3}$ clusters have been attributed then to ionic hydrogen bonds[7a,b] and to a possible proton transfer.[7c]

The other goals to study the hydrated superoxide clusters are of a more practical value. As known,[8] superoxide hydrates are observed in water vapor that contains traces of hydrogen peroxide and in atmosphere. The structural aspect of water surrounding anions is of major importance in chemistry and biology[9] due to the profound effect of their microhydration on reactivity. Interestingly, as quite recently demonstrated,[10] superoxide hydrates are the basic ingredients in silicic water used as drinking water with striking medical properties.

The present work undertakes the aim of a thorough, high-level computational investigation of the lower energy potential energy surfaces (PESs) of the $O_2^-(H_2O)_n$ ($n = 1-4$) complexes in order to demonstrate the key structural and energetic features of the formation of such clusters and the energetics of their

* Corresponding author. Phone: +32 (4) 3662 342. Fax: +32 (4) 3663 413. E-mail: eugene.kryachko@ulg.ac.be.
[†] Bogoliubov Institute for Theoretical Physics.
[§] University of Liege.

10.1021/jp046498z CCC: $30.25
Published on Web 03/11/2005

TABLE 1: Energies, Enthalpies, Entropies, ZPVEs, and Rotational Constants of the $O_2^-(H_2O)_{1,2}$ Species Calculated at the B3LYP/A and QCISD/B (indicated by the superscript ∗) Computational Levels

					rotational constants, MHz		
	−energy, hartree	ZPVE, kcal/mol	−enthalpy, hartree	entropy, cal/mol·T	*A*	*B*	*C*
$\mathbf{I}_1$	226.88482	16.85	226.85319	69.76	36649.0016	5768.7914	4984.2396
	226.24291*	17.04*	226.21094*	69.68*	33624.7336*	5876.2902*	5002.1158*
$\mathbf{I}^{ts}_1$	226.88400	17.00	226.85286	64.77	32766.9450	6414.1310	5364.1068
	226.24184*	17.24*	226.21017*	65.48*	31976.6992*	6263.0817*	5237.2863*
$\mathbf{I}_2$	303.37252	32.38	303.31312	87.59	33503.8693	1827.8339	1733.2731
	302.51305*				31123.3189*	1862.1577*	1757.0317*
$\mathbf{II}_2$	303.37227	32.94	303.31265	83.07	5441.5311	4496.6444	2487.0154
	302.51174*				5454.3333*	4316.8947*	2441.4104*
$\mathbf{III}_2$	303.37203	32.47	303.31245	87.79	20373.8923	1985.1023	1808.8587
	302.51337*				23197.5309*	1938.3232*	1788.8516*
$\mathbf{IV}_2$	303.36724	32.61	303.30777	85.90	6322.7045	3575.7647	2451.1261
	302.50914*				6153.3615*	3628.2422*	2513.8813*
$\mathbf{V}_2$	303.30201	32.32	303.24361	80.55	7991.4925	4215.7522	2909.3236
$\mathbf{I}_2^{ts1}$	303.37164	32.37	303.31291	84.03	26629.6351	1966.1354	1830.9515
$\mathbf{I}_2^{ts2}$	303.36993	31.99	303.31172	85.33	26589.7918	1737.1338	1630.6052
$\mathbf{II}_2^{ts1}$	303.37136	32.46	303.31291	81.88	5151.6945	4606.8680	2459.8762
$\mathbf{II}_2^{ts2}$	303.37021	32.38	303.31191	81.64	5289.5244	4552.7443	2446.7786
$\mathbf{II}_2^{ts3}$	303.36500	31.52	303.30711	87.72	8913.3539	2191.3025	1844.6070
$\mathbf{III}_2^{ts}$	303.36956	32.02	303.31126	85.93	10643.7098	2149.2692	1788.1838
$\mathbf{IV}_2^{ts}$	303.36684	32.20	303.30853	83.44	4863.8846	3896.0187	2266.2521

mutual interconversions. The computational methodology is outlined in refs 11−14.

2. Structure and Properties of Clusters $O_2^-(H_2O)_{1\le n\le 4}$

2.1. Monohydrated Superoxide as a Reference System. As already mentioned in the Introduction, the superoxide monohydrate has received a great deal of attention in the past.[5−7] That is why in the present work it is treated as a reference system although its specific features, relevant for a further study of $O_2^-(H_2O)_{2\le n\le 4}$, are thoroughly discussed. The planar (C_s) global minimum structure $\mathbf{I}_1$ of $O_2^-\cdot H_2O$ with a single water molecule, hydrogen-bonded to O_2^- on one side, is displayed in Figure 1. Its binding energy amounts to 21.7 [21.2] kcal/mol (the UQCISD/B value is given in square brackets to distinguish it from the ZPVE-corrected value reported hereafter in parentheses) that reduces to 19.9 [19.4] kcal/mol after ZPVE correction (see Table 1). The latter are well correlated with the experimental value of 19.6 ± 1 kcal/mol obtained from photodetachment studies by Luong et al.[7f] and the theoretical ones, 19.15 kcal/mol (B3LYP/aug-cc-pVDZ[7d]), −19.60 kcal/mol (B3LYP/6-311++G(3d,3p)+diffs(sp,s)[6e]), and 19.44 kcal/mol (MP2/6-311++G(3d,3p)+diffs(2s2p,s)[6e]). The magnitude of the binding energy places $\mathbf{I}_1$ into the class of moderate-strong (partially ionic) hydrogen-bonded systems[15,16] that will be later confirmed by a red shift that the stretching mode $\nu(O_3-H_4)$ undergoes under formation of the hydrogen bond $O_3-H_4\cdots O_1$. The enthalpy of the formation of $\mathbf{I}_1$, being equal to −20.1 [−19.7] kcal/mol (Table 1), agrees fairly well with the experimental value (−18.4 kcal/mol) reported about 30 years ago by Arshadi and Kebarle.[8]

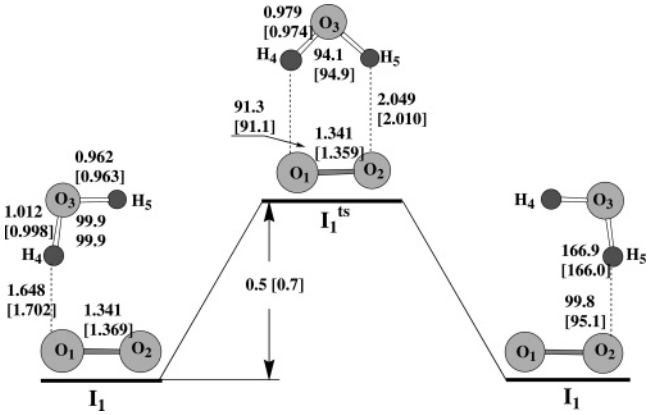

Figure 1. The energetic bottom of the PES of the superoxide monohydrate calculated at the UB3LYP/A and UQCISD/B computational levels (the UQCISD/B values are given in square brackets). Bond lengths are given in Å, bond angles in deg, and energies in kcal/mol.

Figure 1 shows a spectacular elongation of the O_3-H_4 bond by 0.050 [0.036] Å accompanied by a substantial shrink of the $H_4O_3H_5$ bond angle of the water molecule by 5.1° [5.6°] (cf. ref 13). The hydrogen bond $O_3-H_4\cdots O_1$, formed between H_2O and O_2^-, is characterized by an H-bond length of 1.648 [1.702] Å and a bond angle of 166.9° [166.0°]. The former is shorter by ∼ 0.1−0.2 Å compared to that in neutral water clusters. This contraction occurs due to a charge transfer from the SOMO π^*, where the excess electron resides in superoxide, to the σ MO of the neighboring O_3-H_4 bond, which makes the resultant hydrogen bond $O_3-H_4\cdots O_1$ partially ionic and less repulsive to the other hydrogen atom H_5. The latter in turn decreases the bond angle $\angle H_4O_3H_5$. It is also worth mentioning that the angle $\angle O_2O_1H_4$ of 99.8° [95.1°] is the optimal for an efficient $\pi^* \Longrightarrow \sigma$ charge transfer.

The geometrical changes which occur in the water molecule under its bonding to O_2^- naturally affect its spectrum. For example, one observes a blue shift by 129 [116] cm^{-1} of the mode ν_2[15] caused by a shrinking of the $H_4O_3H_5$ angle. The stretching mode ν_1 of the water molecule is significantly downshifted by 872 [644] cm^{-1} and enormously enhanced in IR implying thus that $\mathbf{I}_1$ belongs to the class of the strong (ionic) hydrogen-bonded (IHB) systems. (In $\mathbf{I}_1$, the stretch ν_1 is predicted at 2943 (1555) [3231 (1203)] cm^{-1} and ν_3 at 3866 (10) [3932 (16)] cm^{-1} (IR activity is indicated in parentheses).)

There obviously exist two isomers of $\mathbf{I}_1$ which differ from each other by the bonding of one water molecule to one or another oxygen of superoxide. Its mutual conversion, viewed as a sort of "water rocking", is governed by the transition state $\mathbf{I}_1^{ts}$ of the C_{2v}-symmetry $^2A_2$ placed 0.5 [0.7] kcal/mol higher (see Figure 1 and Table 1). This small barrier height, comparable with *kT*, cannot prevent a nearly "free" jumping between those isomers. However, due to the entropy difference of $\mathbf{I}_1$ and $\mathbf{I}_1^{ts}$ of ∼5 cal/(mol·T), the Gibbs free energy of "water rocking" increases as *T* increases. At $T = 298.15$ K, for example, the

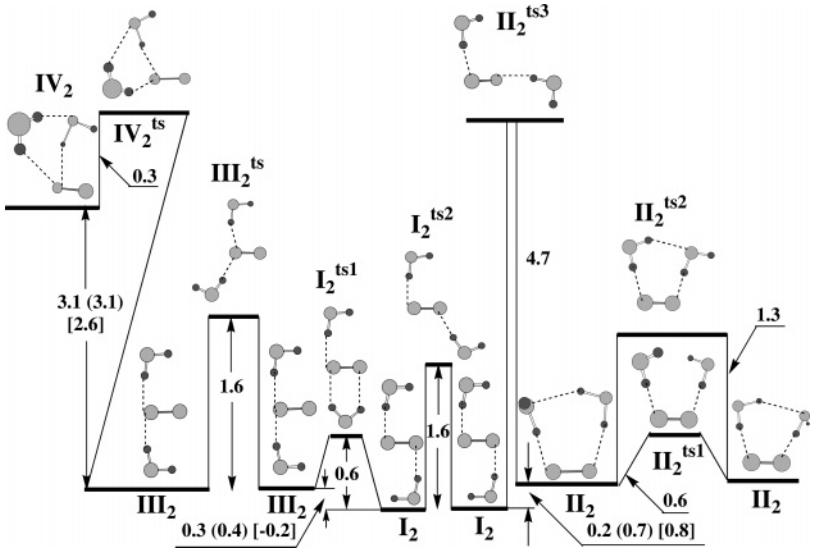

Figure 2. The lower energy portion of the PES of the superoxide dihydrate calculated at the UB3LYP/A and UQCISD/B computational levels (the latter is only confined to the stable species; the UQCISD/B values are given in square brackets). The UB3LYP/A energies after ZPVE corrections are indicated in parentheses. Energies are given in kcal/mol.

Gibbs free energy amounts to 1.7 [1.7] kcal/mol. Hence, the entropy effect hampers the accessibility of the transition state $\mathbf{I}_1^{ts}$ at higher temperatures.

2.2. The Superoxide Dihydrate. We predict three different minimum-energy structures, $\mathbf{II}_2-\mathbf{IV}_2$, on the lower energy portion of the PES of $O_2^-(H_2O)_2$ placed within ~3 kcal/mol above the global minimum of $\mathbf{I}_2$ (see Figure 2). Their properties are surveyed in Table 1 and their optimized geometries calculated at both UB3LYP/A and UQCISD/B computational levels are shown in Figure 3.

The planar global-minimum structure $\mathbf{I}_2$ refers to the $^2A''$ state of the C_s symmetry and has two water molecules bound to different oxygens of superoxide on opposite sides and thereby not bound to each other via the hydrogen bond, typical for the water dimer.[7a,b,d] Its binding energy, taken with respect to the asymptote $\mathbf{I}_1 + H_2O$, amounts to 18.3 [18.0] (16.1) kcal/mol (compare with 17.26 kcal/mol in ref 7d), whereas relative to $O_2^-(X^2\Pi_g) + 2H_2O$, it is equal to 40.0 [39.3] (36.0) kcal/mol. The latter value is about 4 kcal/mol lower than the double former one. This implies that a charge transfer of the excess electron of O_2^- to two separated water molecules is less efficient compared with that to a single water molecule. A reason is the existence of a strong Coulomb repulsion between two negative charges which are localized on the two hydrogen bonds in $\mathbf{I}_2$ and separated from each other by 3.867 [3.896] Å. A rough estimate of such Coulomb repulsion based on Mulliken charges yields ca. 13 kcal/mol. A straightforward comparison of Figures 1 and 3 indicates the following. First, the oxygen−oxygen bond in superoxide undergoes a further contraction, by 0.003 [0.013] Å, compared to that in $\mathbf{I}_1$. Hence, there is a small additional charge transfer. Second, the H···O bond lengths are simultaneously elongated by 0.065 [0.086] Å due to the Coulomb repulsion whereas the O−H bonds are contracted by 0.013 [0.011] Å. Therefore, the hydrogen bonds in $\mathbf{I}_2$ are less ionic compared to those in $\mathbf{I}_1$.

As shown in Figure 2, the other two structures, $\mathbf{II}_2$ and $\mathbf{III}_2$, are placed ≤0.3 kcal/mol above $\mathbf{I}_2$ at the UB3LYP/A level (cf. with ~0.7 kcal/mol in ref 7d). The UQCISD/B level negligibly corrects this order, slightly favoring $\mathbf{III}_2$ over $\mathbf{I}_2$ by 0.2 kcal/mol and slightly disfavoring $\mathbf{II}_2$ by placing it 0.8 kcal/mol higher compared to the UB3LYP/A. (Precisely speaking, we have to assume that these energy difference values are within the computational error margin and therefore all aforementioned structures are nearly isoenergetic.) By analogy with $\mathbf{I}_2$, $\mathbf{III}_2$ is not of a water-dimer type since its two water molecules form hydrogen bonds with the same oxygen atom of superoxide playing the role of a double acceptor (Figure 3). $\mathbf{I}_2$ and $\mathbf{III}_2$ are linked to each other via the transition structure $\mathbf{I}_2^{ts1}$ determining the barrier of 0.9 kcal/mol. It is evident that such a small barrier becomes more or less "transparent" at ambient temperatures; therefore, the interconversion $\mathbf{I}_2 \leftrightarrow \mathbf{III}_2$ is highly probable and this may affect the spectra of dihydrated superoxide as temperature increases.

In contrast to the global-minimum structure, the structure $\mathbf{II}_2$ belongs to a water-dimer type since its two water molecules form the intermolecular hydrogen bond. Its binding energy amounts to 34.0 (31.8) kcal/mol. It is also demonstrated in Figure 2 that the barrier of the conversion of $\mathbf{I}_2$ into $\mathbf{II}_2$, governed by the transition-state linker $\mathbf{II}_2^{ts3}$, is equal to 4.7 (3.9) kcal/mol (see Figure 1S of the Supporting Information for the optimized geometry of $\mathbf{II}_2^{ts3}$). Hence, this reaction route is less probable than that existing between $\mathbf{I}_2$ and $\mathbf{III}_2$. Also notice the existence of the interesting transition state $\mathbf{II}_2^{ts1}$ which determines a lower energy intraconversion (0.6 kcal/mol) of the dimer hydrogen bond. Its structure displayed in Figure 1S of the Supporting Information includes a pair of opposite and out-of-plane hydrogen atoms separated from each other by 2.219 Å.

The fourth lower energy conformer $\mathbf{IV}_2$ structurally resembles $\mathbf{III}_2$. However, its two water molecules form a relatively weak, strongly nonlinear hydrogen bond characterized by a $H_5\cdots O_4$ bond length equal to 2.130 [2.179] Å and a bond angle $\angle O_3H_5O_4 = 146.4°$ [143.9°]. Overall, this means that the formation of superoxide dihydrate from superoxide monohydrate somewhat preferentially proceeds via sequential monohydration, either via $\mathbf{I}_2$ or $\mathbf{III}_2$, rather than via a direct hydration by water dimer throughout $\mathbf{II}_2$. We assume that $\mathbf{IV}_2$ is intermediate between these two remarkedly different classes although, to a lesser extent, it could be referred to the latter one.

Inspecting Figure 3 we find that one donating O_4-H_6 bond of the water dimer either in $\mathbf{II}_2$ or in $\mathbf{IV}_2$ is strongly elongated by ~0.080 Å relative to water monomer, on one hand, and on the other, it is slightly elongated by ~0.006−0.008 Å compared to that in superoxide monohydrate $\mathbf{I}_1$. This indicates its larger ionic character which, as we suggest, occurs due to two

Figure 3. The optimized geometries of the lower energy structures of $O_2^-(H_2O)_{2\le n\le 4}$ calculated at the UB3LYP/A level (including the UQCISD/B computational level for $n = 2$ in square brackets). Bond lengths are given in Å and bond angles in deg.

effects: a charge transfer from superoxide (a donating hydrogen bond) and a charge transfer from another water molecule due to formation of the water−water hydrogen bond (accepting hydrogen bond). Altogether, this results in a significant red shift (ca. 1100 cm^{-1}) of the corresponding OH stretching mode appearing at 2807 cm^{-1} in $\mathbf{II}_2$ and at 2784 cm^{-1} in $\mathbf{IV}_2$. The structure $\mathbf{II}_2$ has recently been assigned by Johnson and co-workers[7a,b] as the only one that provides a signal of the inter-water H-bonded OH fundamental mode in their experimental spectrum. This implies that under the conditions of the experiment conducted by Johnson and co-workers,[7a,b] this structure is highly populated. In contrast, the red shifts of the harmonic stretching modes ν_1 of water molecules in structures $\mathbf{I}_2$ and $\mathbf{III}_2$ are less pronounced (ca. 700 cm^{-1}). These two modes are coupled to each other and manifested as the doublet $\nu_1^{sym} = 3154$ (2589) cm^{-1} and $\nu_1^{asym} = 3200$ (0) cm^{-1} for $\mathbf{I}_2$ and $\nu_1^{sym} = 3229$ (2187) cm^{-1} and $\nu_1^{asym} = 3295$ (27) cm^{-1} for $\mathbf{III}_2$.

2.3. The Lower Energy Portion of the PES of $O_2^-(H_2O)_3$. In Figure 1C of ref 7a (see also Figure 3 in ref 7d and Figure 1 in ref 7e), Johnson and co-workers demonstrate that superoxide, bonded to three water molecules, is remarkedly distinct from its mono- and dihydrated analogues. By contrast, its spectrum is comprised of two well-separated (of about 300 cm^{-1}) strong bands, both assigned to the ionic hydrogen bonds.[7a] Let us note as well that the shape of the second band that is placed at higher wavenumbers precisely mimics that of the band observed for the dihydrated superoxide.

In Figure 3 we display six different lower energy structures lying on the PES of $O_2^-(H_2O)_3$. The hydrogen-bonded patterns of the two most stable and isoenergetic structures, $\mathbf{I}_3$ and $\mathbf{II}_3$, obey a simple rule **1d2d + 3d = 1d^{2}2d3ad**.[18] The latter demonstrates that $\mathbf{I}_3$ is formed either via $\mathbf{III}_2 + H_2O$ or via $\mathbf{II}_2 + H_2O$ as a less energetically favorable route whereas $\mathbf{II}_3$ via $\mathbf{I}_2 + H_2O$ or $\mathbf{II}_2 + H_2O$. Relative to the asymptote $\mathbf{I}_2 + H_2O$, the binding energies of $\mathbf{I}_3$ and $\mathbf{II}_3$ correspondingly amount to 15.7 and 13.0 kcal/mol (after ZPVE).

Upon geometrical comparison of the $\mathbf{I}_3$ and $\mathbf{II}_3$ structures with their dihydrate analogues $\mathbf{I}_2$ and $\mathbf{II}_2$, one observes a weakening of all hydrogen bonds between water molecules and superoxide: the relevant O−H bond lengths are contracted by ∼0.01 Å (**2d**) to 0.02 Å ($\mathbf{1d}_i$ in comparison with those in $\mathbf{I}_2$) and by ∼0.01 (**3d**) in comparison with that in $\mathbf{II}_2$. All their H···O bond lengths are elongated by 0.05−0.07 Å. In contrast, the intermolecular hydrogen bond in the water dimer is strenghtened: the H ···O bond length decreases by 0.01 Å. In other words, the trihydrate superoxide shows a clear tendency to be closer

TABLE 2: The B3LYP/A Energies, Enthalpies, Entropies, ZPVEs, and Rotational Constants of the $O_2^-(H_2O)_{3,4}$[a]

					rotational constants, MHz		
	−energy, hartree	ZPVE, kcal/mol	−enthalpy hartree	entropy, cal/mol·T	*A*	*B*	*C*
$\mathbf{I}_3$	379.85611 378.77817*	48.48	379.76850	101.44	5349.4984	1410.9780	1122.3726
$\mathbf{II}_3$	379.85611 378.77878*	48.48	379.76848	101.63	5327.2731	1422.2847	1127.7186
$\mathbf{III}_3$	379.85228 378.77449*	47.81	379.76532	106.80	9046.5038	893.5025	846.5990
$\mathbf{IV}_3$	379.85275 378.77500*	48.88	379.76490	99.72	3077.9659	2326.4813	1817.2701
$\mathbf{V}_3$	379.85328 378.77652*	49.39	379.74698	95.43	2987.8686	2464.1160	2300.7034
$\mathbf{VI}_3$	379.84953 378.77344*	48.56	379.76189	100.38	2900.5701	2699.0539	1524.2319
$\mathbf{I}_4$	456.33752 455.04287*	64.56	456.22165	115.54	2957.8921	1004.3192	759.3551
$\mathbf{II}_4$	456.33504 455.03996*	63.99	456.21962	120.59	2797.5525	792.4164	648.8334
$\mathbf{III}_4$	456.33503 455.04251*	64.84	456.21883	114.61	2844.7340	1057.0924	1024.8763
$\mathbf{IV}_4$	456.33424 455.03904*	64.00	456.21886	120.65	3778.0861	671.2890	604.5099
V4	456.33453 455.04132*	65.65	456.21792	107.16	2074.9734	1687.0303	1386.2835
$\mathbf{VI}_4$	456.33094 455.03553*	63.27	456.21626	126.79	7573.8584	476.9207	458.6322

[a] Their energies are further refined at the QCISD/B//B3LYP/A level (indicated by the superscript ∗).

TABLE 3: Selected B3LYP/A Vibrational Modes of the $O_2^-(H_2O)_3$ Structures $\mathbf{I}_3-\mathbf{VI}_3$[a]

	$\mathbf{I}_3$	$\mathbf{II}_3$	$\mathbf{III}_3$	$\mathbf{IV}_3$	$\mathbf{V}_3$	$\mathbf{VI}_3$
$\nu_{O_2^-}$	1202	1199	1193	1199	1193	118
ν_2	1670 (89) O_4	1670 (91) O_2	1683 (170) O_5	1651 (59) O_9	1695 (139) O_5	1687 (33) O_9
	1709 (185) asym $O_{1,10}$	1711 (204) O_{10}	1714 (164) O_4	1703 (193) O_1	1700 (80) asym $O_{1,2}$	1697 (116) asym $O_{1,6}$
	1733 (108) sym $O_{1,10}$	1731 (65) O_4	1742 (32) O_1	1742 (91) O_4	1732 (109) sym $O_{1,2}$	1713 (148) sym $O_{1,6}$
ν_{IHB}	3032 (1594) H_8	3085 (1564) H_5	2832 (2341) H_6	2959 (1202) H_{10}	3147 (532) asym $H_{9,10}$	3141 (1264) asym $H_{4,8}$
	3359 (1047) H_9	3359 (1009) H_9	3256 (989) H_9	3308 (879) H_8	3283 (1219) sym $H_{9,10}$	3248 (786) sym $H_{4,8}$
	3513 (508) H_5	3482 (572) H_8	3420 (781) H_{10}			
ν_{IW}	3743 (176) H_6	3748 (168) H_7		3621 (286) H_7	3755 (128) H_8	3645 (206) sym $H_{10,11}$
				3712 (186) H_7	3808 (75) H_{11}	3706 (453) asym $H_{10,11}$
ν_{WHB}				3757 (169) H_5	3716 (193) H_6	
ν_3	3869 (17) H_{11}	3870 (19) H_{11}	3872 (35) H_7	3868 (19) H_{11}		3858.9 (44) asym $H_{5,7}$
	3875 (20) H_7	3876 (20) H_6	3873 (9) H_8			3859.4 (2) sym $H_{5,7}$
			3877 (26) H_{11}			

[a] $\nu_{O_2^-}$ refers to the O−O stretching mode of superoxide, ν_2 to the scissor mode of the water molecule, ν_{IHB} to the stretch of ionic hydrogen bond, ν_{IW} to that of the interwater hydrogen bond, ν_{WHB} to a weak water−superoxide hydrogen bond, and ν_3 to the stretch of "free" OH groups. Frequencies are given in cm^{-1} and IR activities (in parentheses) in km/mol.

to the "border" between the ion−water and water−water interactions than its dihydrate, as though its representative structures, $\mathbf{I}_3$ and $\mathbf{II}_3$, are placed on the ion−water side because all three of their water molecules are bound to superoxide via a sort of ionic hydrogen bond. These geometrical changes which occur under formation of $\mathbf{I}_3$ and $\mathbf{II}_3$ by binding a third water molecule either to $\mathbf{I}_2$ or to $\mathbf{III}_2$ result in blue shifts (150−200 cm^{-1}) of the stretching modes associated with the water−superoxide hydrogen bonds (see Table 3). It may explain the origin of the second absorption band IHB_2 and its shift to higher wavenumbers, ∼3050−3250 cm^{-1}, with retaining its shape.

What then is the origin of the first absorption band IHB_1 at ca. 2800 cm^{-1} (Figure 1C, ref[7a]) whose shape is different from that in the spectra of mono- and dihydrated superoxide? Why does it appear for the first time when three water molecules are bound to superoxide? We suggest that it might be rooted to the structure $\mathbf{III}_3$ placed closer to the "border" between the ion−water and water−water interactions in a sense that it is formed via bonding of a third water molecule of $O_5H_{10}H_{11}$ to $\mathbf{I}_2$, rather than to superoxide. We may suggest the existence of two concordant effects. One of them is related to a charge transfer from the superoxide molecule to the $O_1-H_6\cdots O_2$ bond that makes it ionic. The other is due to an increase of the proton acceptor character of the oxygen O_1. The latter in turn strengthens its hydrogen bonding with the water molecule $O_5H_{10}H_{11}$ and, thanks to an additional charge transfer, facilitated due to its practical linearity ($\angle O_5H_{10}H_{11} = 173.7°$), also strengthens the $O_1-H_6\cdots O_2$ bond. This is indicated by lengthening of the O_1-H_6 bond by 0.018 Å and by compressing of the $H_6\cdots O_2$ distance by 0.117 Å, compared to that in $\mathbf{I}_2$. The latter is indeed the smallest H···O distance between the hydrogen atom and superoxide, among all studied lower energy structures of trihydrated superoxide. Hence, the H-bond $O_1-H_6\cdots O_2$ is the strongest ionic-type hydrogen bond existing in the $O_2^-(H_2O)_{1\le n\le 3}$ clusters. Summarizing, the structure $\mathbf{III}_3$ exhibits a quite interesting balance between the ion−water and water−water interactions related, first, to the donor−acceptor motif of the effect of cooperativity in hydrogen bonding (see also refs 15−17) and, second, to the question of whether the "border" between the ion−water and water−water interactions is so well-defined? On one hand, $\mathbf{III}_3$ favors a third water molecule to be bonded to the single-water core of $\mathbf{I}_2$, showing thus a preference to the water−water interaction rather than to the ion−water.[19] On the other, an additional third molecule in $\mathbf{III}_3$ significantly strengthens the ion−water interaction within the single-water core of $\mathbf{I}_2$ that enhances an ionic character of

TABLE 4: Selected B3LYP/A Vibrational Modes of the $O^-_2(H_2O)_4$ Structures I_4−VI_4[a]

	I_4	II_4	III_4	IV_4	V_4	VI_4
$\nu_{O_2^-}$	1212	1204	1196	1205	1194	1197
ν_2	1659 (1) sym $O_{5,12}$	1662 (111) O_{12}	1692 O_1	1669 (77) O_4	1686 (26) $O_{4,5,12}$	1678 (305) asym $O_{9,12}$
	1681 (179) asym $O_{5,12}$	1677 (119) O_1	1703 (152) sym $O_{4,5}$	1679 (159) O_5	1700 (99) sym $O_{4,5}$	1681 (0) sym $O_{9,12}$
	1716 (95) asym $O_{1,4}$	1708 (148) O_5	1706 (173) asym $O_{4,5}$	1720 (133) asym $O_{1,12}$	1706 (134) asym $O_{4,5}$	1726 (137) asym $O_{1,6}$
	1728 (150) sym $O_{1,4}$	1748 (70) O_4	1724 (44) sym $O_{1,4,5,12}$	1736 (90) sym $O_{1,12}$	1723 (114) $O_{1,5,12}$	1742 (0) sym $O_{1,6}$
ν_{IHB}	3163 (2104) asym $H_{9,13}$	3078 (1245) H_{13}	3287 (701) H_9	3077 (3159) asym $H_{9,13}$	3200 (1042) H_9	2912 (4030) asym $H_{4,8}$
	3235 (509) sym $H_{9,13}$	3307 (2110) sym $H_{7,9}$	3395 (1607) asym $H_{10,13}$	3135 (86) sym $H_{9,13}$	3389 (151) asym $H_{6,13}$	2990 (0) sym $H_{4,8}$
	3553 (1078) asym $H_{6,10}$	3401 (325) H_{10}	3443 (119) sym $H_{10,13}$		3441 (1013) sym $H_{6,13}$	
	3580 (62) sym $H_{6,10}$	3447 (692) asym $H_{7,9}$				
ν_{IW}	3746 (59) asym $H_{7,11}$	3700 (243) H_8	3600 (325) H_7	3471 (691) H_{11}	3603 (134) sym $H_{10,11}$	3449 (1472) asym $H_{10,13}$
	3748 (303) sym $H_{7,11}$		3744 (149) H_8	3559 (519) H_6	3665 (531) asym $H_{10,11}$	3450 (0) sym $H_{10,13}$
			3776 (88) H_6	3742 (186) H_7	3706 (232) H_7	
			3791 (130) H_{14}		3724 (211) H_{14}	
ν_3	3877.4 (46) asym $H_{8,14}$	3873 (22) H_{11}	3870 (20) H_{11}	3870 (29) H_{14}	3867 (28) H_8	3874.5 (59) asym $H_{5,7}$
	3877.9 (10) sym $H_{8,14}$	3877 (24) H_{14}		3876 (24) H_8		3874.8 (≈1) sym $H_{5,7}$
		3880 (28) H_6		3879 H_{10}		3879 (17) sym $H_{11,14}$
				3879 (36) asym $H_{11,14}$		

[a] $\nu_{O_2^-}$ refers to the O−O stretching mode of superoxide, ν_2 to the scissor mode of the water molecule, ν_{IHB} to the stretch of the ionic hydrogen bond, ν_{IW} to that of the interwater hydrogen bond, ν_{WHB} to a weak water−superoxide hydrogen bond, and ν_3 to the stretch of "free" OH groups. Frequencies are given in cm^{-1} and IR activities (in parentheses) in km/mol.

one of its hydrogen bonds, viz., $O_1-H_6\cdots O_2$. It is this hydrogen bond $O_1-H_6\cdots O_2$ whose stretching mode falls around 2800 (2832 cm^{-1} is the theoretical estimate for harmonic frequency) cm^{-1} (see Table 3). Furthermore, structurally speaking, $\mathbf{III}_3$ supports a viewpont that both interactions, ion−water and water−water, are strongly Coulomb correlated in hydrated anionic superoxide complexes in a manner that, while accepting a hydrogen bond from another water molecule, a given water molecule donates more strongly its proton to anion. The latter is precisely the aforementioned donor−acceptor motif of the hydrogen-bonding cooperativity effect, which hence rules out a sharp "border" between these two interactions in the studied complexes.

Speaking rather in energy terms, the structure $\mathbf{III}_3$ lies 1.7 kcal/mol (after ZPVE) higher than $\mathbf{I}_3$. However, due to a large entropy effect (see Table 2), their Gibbs free energy difference reduces to −0.4 kcal/mol at $T = 298.15$ K. On one hand, the latter magnitude allows us to consider three structures, $\mathbf{I}_3$ ($\mathbf{II}_3$) and $\mathbf{III}_3$, as nearly isoenergetic. On the other, it underlies a somewhat temperature dependence of the first absorption band IHB_1.

The title PES also includes another three structures $\mathbf{IV}_3$−$\mathbf{VI}_3$ placed correspondingly 2.5, 2.7, and 4.2 kcal/mol, after ZPVE, higher than the global minimum (see Figure 3). The former two evidently originated from $\mathbf{II}_2$ whereas the latter is a novel cyclic structure that is formed by the ring-type water trimer bonded to superoxide. Interestingly, $\mathbf{VI}_3$ has the longest superoxide bond of 1.340 Å among the studied structures. This explains a blue shift by 18 cm^{-1} of the ν(O−O) stretching mode.

2.4. Lower Energy Structures of Tetrahydrated Superoxide. The lower energy portion of the PES of $O_2^-(H_2O)_4$, displayed in Figure 3, is comprised of six different structures. Their basic properties are collected in Tables 2 and 4. The most stable structure $\mathbf{I}_4$, earlier reported by Johnson and co-workers,[7a] is composed of two water dimers symmetrically bound to the superoxide molecule on its opposite sides via two ionic and two moderate hydrogen bonds. Its hydrogen-bond pattern resembles those pertaining to the structure $\mathbf{II}_2$. Pursuing further this analogy, we ascribe the hydrogen bonds $O_5-H_9\cdots O_3$ and $O_{12}-H_{13}\cdots O_3$ formed between water molecules of the **da**-type and superoxide to the class of moderate-strong (partially ionic) bonds.[15,16] They are characterized by r(O−H) = 0.997 Å, r(H···O) = 1.708 Å, and the bond angle of 175.0°. Their stretching modes are strongly coupled and exhibit the doublet IHB_1, centered at 3163 (2104 km/mol) and 3235 cm^{-1} (509 km/mol), with the IR activity ratio of 2104/509 ≈ 4.1. After taking anharmonic effects into account, it definitely corresponds to the experimental IR band of the spectrum of the tetrahydrated superoxide observed by Johnson and co-workers in the region of 2900−3150 wavenumbers (see Figure 2 in ref 7a).

The other two hydrogen bonds, which superoxide forms with water molecules of the **dd**-type in $\mathbf{I}_4$, belong to the moderate type. They possess shorter (by 0.019 Å) O−H bonds compared to the ionic ones, and, in contrast, their H···O lengths are longer by 0.224 Å. However, by analogy with the ionic bonds, the stretching modes of these two hydrogen bonds are also strongly coupled and develop into the symmetric (at 3553 cm^{-1} (1078 km/mol)) and asymmetric modes (3580 cm^{-1} (62 km/mol)) (see the IR band IHB_2 in Figure 2 of ref 7a), undergoing thus the red shift of ≈260−300 wavenumbers. The latter estimate is typical for normal weak hydrogen bonds. Additionally, there exist the other four harmonic stretching vibrations. Two of them, giving rise to the IW band, which is shown in Figure 2 of ref 7a, peaked at 3746 cm^{-1} (59 km/mol) and 3748 cm^{-1} (303 km/mol) and are assigned to the asymmetric and symmetric stretches of weakly bound water dimers. The other two, appearing at 3877.4 and 3877.9 cm^{-1} and describing the stretches of "free" OH groups of the **da**-type water molecules, form the IR band F.

A remaining part of the title portion of the PES consists of the structures $\mathbf{II}_4$−$\mathbf{VI}_4$ lying higher than $\mathbf{I}_4$, viz, $\mathbf{II}_4$ by 1.6 (1.0) kcal/mol, $\mathbf{III}_4$ by 1.6 (1.8) kcal/mol, $\mathbf{IV}_4$ by 2.1 (1.5) kcal/mol, $\mathbf{V}_4$ by 1.9 (3.0) kcal/mol, and finally $\mathbf{VI}_4$ by 4.1 (2.8) kcal/mol (cf. also their UQCISD/B//UB3LYP/A energies collected in Table 2). Due to a large entropy effect, the structure $\mathbf{II}_4$ becomes slightly more favorable, by 0.2 kcal/mol, in terms of Gibbs free energy than $\mathbf{I}_4$ at room temperature. $\mathbf{VI}_4$ appears then nearly isoenergetic (with a tiny difference of 0.03 kcal/mol) to $\mathbf{I}_4$. Interestingly, the structure $\mathbf{III}_4$ has a typical water trimer bonded to superoxide by its free OH groups.

3. Summary and Conclusions

We have performed a detailed investigation of the lower energy portions of the potential energy surfaces of $O_2^-(H_2O)_{1\le n\le 4}$ and found four stable structures for the superoxide dihydrate and six for $O_2^-(H_2O)_3$ and $O_2^-(H_2O)_4$. The structural, energetic, and spectroscopic features of these stable superoxide hydrates

have been discussed. Their hydrogen bond patterns also have been studied in order to partially shed a light on which type of interaction, the anion−water or water−water, is preferential in these clusters. We have presented the arguments supporting the viewpoint that the effect of cooperativity of hydrogen bonding blurs a sharp "border" between these two interactions. For the first time, the present work has reported the transition-state linkers between the most stable superoxide hydrates that certainly will be useful in understanding the mechanism of their interconversions.

Acknowledgment. One of the authors, E.S.K., gratefully thanks Francoise Remacle for warm hospitality. This work was supported by the Region Wallonne (RW. 115012) and the F.R.F.C. 2.4562.03F (Belgium) and the computational facilities of NIC (University of Liege) were used. We also thank the reviewer for valuable comments and suggestions.

Supporting Information Available: The optimized geometries of the superoxide dihydrate transition state structures obtained at the UB3LYP/A and UQCISD/B computational levels (the UQCISD/B values are given in square brackets) are displayed in Figure 1S (bond lengths are given in Å and bond angles in deg). This material is available free of charge via the Internet at http://pubs.acs.org.

References and Notes

(1) (a) Grisham, M. B.; McCord, J. M. In *Physiology of Oxygen Radicals*; Taylor, A. E., Matalon, S., Ward, P. A., Eds.; Waverly Press: Baltimore, MD, 1986; p 1 ff. (b) Ames, B. N.; Shigenaga, M. K.; Hagan, T. M. *Proc. Natl. Acad. Sci. U.S.A.* **1993**, *90*, 7915. (c) Gotz, M. E.; Kunig, G.; Riederer, P.; Youdim, M. B. *Pharmacol. Ther.* **1994**, *63*, 37. (d) Lovell, M. A.; Xie, C.; Markesbery, W. R. *Brain Res.* **2000**, *855*, 116. (e) Schöneich, C. *Exp. Gerontol.* **1999**, *34*, 19. (f) Nicholls, D. G.; Ferguson, S. J. *Bioenergetics 2*; Academic: San Diego, CA, 1992. (g) Adams, A. *The Scientist* **2002**, *16*, 30. (h) Moskovitz, J.; Yim, M. B.; Chock, P. B. *Arch. Biochem. Biophys.* **2002**, *397*, 354. (i) Stadtman, E. R. *Trends Biochem. Sci.* **1986**, *11*, 11. (j) Beckman, K. B.; Ames, B. N. *Physiol. Rev.* **1998,** *78*, 547.

(2) (a) Salvemini, D.; et al. *Science* **1999**, *286*, 304. (b) Reeves, E. P.; Lu, H.; Jacobs, H. L.; Messina, C. G. M.; Bolsover, S.; Gabella, G.; Potma, E. O.; Warley, A.; Roes, J.; Segal, A. W. *Nature* **2002**, *416*, 291 and references therein. (c) Laight, D. W.; Carrier, M. J.; Ånggård, E. E. *Cardiovasc. Res.* **2000**, *47*, 457. (d) Carr, A.; Frei, B. *Free Radical Biol. Med.* **2000**, *28*, 1806. (e) Taddei, S.; Virdis, A.; Ghiadoni, L.; Salvetti, G.; Salvetti, A. *J. Nephrol.* **2000**, *13*, 205. (f) Liochev, S. I.; Fridovich, I. *Arch. Biochem. Biophys.* **2002**, *402*, 166. (g) Chen, H.-Y.; Hu, R.-G.; Wang, B.-Z.; Chen, W.-F.; Liu, W.-Y.; Schröder, W.; Frank, P.; Ulbrich, N. *Arch. Biochem. Biophys.* **2002**, *404*, 218. (h) Ookawara, T.; Kizaki, T.; Takayama, E.; Imazeki, N.; Matsubara, O.; Ikeda, Y.; Suzuki, K.; Ji, L. L.; Tadakuma, T.; Taniguchi, N.; Ohno, H. *Biochem. Biophys. Res. Commun.* **2002**, *296*, 54. (i) Garrison, W. M. *Chem. Rev.* **1987**, *87*, 381.

(3) (a) Keese, R. G.; Lee, N.; Castleman, A. W., Jr. *Geophys. Res.* **1979**, *84*, 3791. (b) Fahey, D. W.; Bohringer, H.; Fehsenfeld, F. C.; Ferguson, E. E. *J. Chem. Phys.* **1982**, *76*, 1799. (c) Yang, X.; Castleman, A. W., Jr. *J. Am. Chem. Soc.* **1991**, *113*, 6766. (d) Ernestova, L. S.; Skurlatov, Y. I. *Zh. Fiz. Khim.* **1995**, *69*, 1159. (e) Paik, D. H.; Bernhardt, T. M.; Kim, N. J.; Zewail, A. H. *J. Chem. Phys.* **2001**, *115*, 612. (f) Meesungnoen, J.; Filali-Mouhim, A.; Ayudhya, N. S. N.; Mankhetkorn, S.; Jay-Gerin, J.-P. *Chem. Phys. Lett.* **2003**, *377*, 419. (g) Flyunt, R.; Leitzke, A.; Mark, G.; Mvula, E.; Reisz, E.; Schick, R.; v. Sonntag, C. *J. Phys. Chem. B* **2003**, *107*, 7242. (h) Hanaoka, K.; Sun, D.; Lawrence, R.; Kamitani, Y.; Fernandes, G. *Biophys. Chem.* **2004**, *107*, 71.

(4) (a) Lavrich, D. J.; Buntine, M. A.; Serxner, D.; Johnson, M. A. *J. Chem. Phys.* **1993**, *99*, 5910. (b) Buntine, M. A.; Lavrich, D. J.; Dessent, C. E.; Scarton, M. G.; Johnson, M. A. *Chem. Phys. Lett.* **1993**, *216*, 471. (c) Lavrich, D. J.; Buntine, M. A.; Serxner, D.; Johnson, M. A. *J. Phys. Chem.* **1995**, *99*, 8453. (d) Desreumaux, J.; Calais, M.; Adriano, R.; Trambaud, S.; Kappenstein, C.; Nguefack, M. *Eur. J. Inorg. Chem.* **2000**, *9*, 2031.

(5) (a) Curtiss, L. A.; Melendres, C. A.; Reed, A. E.; Weinhold, F. *J. Comput. Chem.* **1986**, *7*, 294. (b) Lopez, J. P.; Albright, T. A.; McCammon, J. A. *Chem. Phys. Lett.* **1986**, *125*, 454. (c) Ohta, K.; Morokuma, K. *J. Phys. Chem.* **1987**, *91*, 401. (d) Pilipchuk, V. G.; Smolinskii, V. V.; Shchekatolina, S. A. *Zh. Strukt. Khim.* (*USSR*) **1988**, *29*, 149. (e) Lopez, J. P. *J. Comput. Chem.* **1989**, *10*, 55.

(6) (a) Pilipchuk, V. G.; Smolinskii, V. V.; Shchekatolina, S. A. *Zh. Strukt. Khim.* (*USSR*) **1990**, *31*, 137. (b) Lee, E. P. F.; Dyke, J. M. *Mol. Phys.* **1991**, *74*, 333. (c) Smolinskii, V. V.; Shchekatolina, S. A. *Zh. Strukt. Khim.* (*USSR*) **1992**, *33*, 160. (d) Robinson, E. M. C.; Holstein, W. L.; Stewart, G. M.; Buntine, M. A. *Phys. Chem. Chem. Phys.* **1999**, *1*, 3961. (e) Lee, H. M.; Kim, K. S. *Mol. Phys.* **2002**, *100*, 875. (f) Bell, A. J.; Wright, T. G. *Phys. Chem. Chem. Phys.* **2004**, *6*, 4385.

(7) (a) Weber, J. M.; Kelley, J. A.; Nielsen, S. B.; Ayotte, P.; Johnson, M. A. *Science* **2000**, *287*, 2461. (b) Weber, J. M.; Kelley, J. A.; Robertson, W. H.; Johnson, M. A. *J. Chem. Phys.* **2001**, *114*, 2698. (c) Jørgensen, P.; Forster, J. S.; Hvelplund, P.; Nielsen, S. B.; Tomita, S. *J. Chem. Phys.* **2001**, *115*, 5101. (d) Seta, T.; Yamamoto, M.; Nishioka, M.; Sadakata, M. *J. Phys. Chem. A* **2003**, *107*, 962. (e) Kuo, I.-F. W.; Tobias, D. J. *J. Phys. Chem. A* **2002**, *106*, 10969. (f) Luong, A. K.; Clements, T. G.; Sowa Resat, M.; Continetti, R. E. *J. Chem. Phys.* **2001**, *114*, 3449.

(8) Arshadi, M.; Kebarle, P. *J. Phys. Chem.* **1970**, *74*, 1483.

(9) (a) Takashima, K.; Riveros, J. M. *Mass. Spectrom. Rev.* **1998**, *17*, 409. (b) Desreumaux, J.; Calais, M.; Adriano, R.; Trambaud, S.; Kappenstein, C.; Nguefack, M. *Eur. J. Inorg. Chem.* **2000**, *9*, 2031 and references therein.

(10) (a) Olodovskii, P. P.; Berestova, I. L. *Inzh.-F-z. Zh.* **1992**, *62*, 853. (b) Olodovskii, P. P. *Inzh.-F-z. Zh.* **1992**, *62*, 859. (c) Olodovskii, P. P. *Inzh.-F-z. Zh.* **1992**, *63*, 80. (d) Olodovskii, P. P. *Inzh.-F-z. Zh.* **1994**, *67*, 437. (e) Olodovskii, P. P. *Inzh.-F-z. Zh.* **1995**, *68*, 276. (f) Olodovskii, P. P.; Karpel, O. V. *Inzh.-F-z. Zh.* **2001**, *74*, 141.

(11) All computations were performed at the density functional hybrid UB3LYP potential in conjunction with split-valence 6-311++G(d,p) (≡A) basis set, using the GAUSSIAN 03 suit of packages.[12] The tight convergence criterion was employed in all optimizations with lifting any geometrical constraints. By analogy with ref 6d, the quadratic configuration interaction method, including single and double excitations (UQCISD), was also used with a smaller basis set 6-31+G(d,p) (≡B) to further refine the geometries of the relevant structures. Harmonic vibrational frequencies were kept unscaled. Zero-point vibrational energies (ZPVE) and thermodynamic quantities were also calculated at $T = 298.15$ K. Throughout the present work, the energy comparison was made in terms of the electronic energy + ZPVE. The expectation value $\langle \mathbf{S}^2 \rangle$ was kept at 0.750.

(12) Frisch, M. J.; Trucks, G. W.; Schlegel, H. B.; Scuseria, G. E.; Robb, M. A.; Cheeseman, J. R.; Montgomery, J. A., Jr.; Vreven, T.; Kudin, K. N.; Burant, J. C.; Millam, J. M.; Iyengar, S. S.; Tomasi, J.; Barone, V.; Mennucci, B.; Cossi, M.; Scalmani, G.; Rega, N.; Petersson, G. A.; Nakatsuji, H.; Hada, M.; Ehara, M.; Toyota, K.; Fukuda, R.; Hasegawa, J.; Ishida, M.; Nakajima, T.; Honda, Y.; Kitao, O.; Nakai, H.; Klene, M.; Li, X.; Knox, J. E.; Hratchian, H. P.; Cross, J. B.; Adamo, C.; Jaramillo, J.; Gomperts, R.; Stratmann, R. E.; Yazyev, O.; Austin, A. J.; Cammi, R.; Pomelli, C.; Ochterski, J. W.; Ayala, P. Y.; Morokuma, K.; Voth, G. A.; Salvador, P.; Dannenberg, J. J.; Zakrzewski, V. G.; Dapprich, S.; Daniels, A. D.; Strain, M. C.; Farkas, O.; Malick, D. K.; Rabuck, A. D.; Raghavachari, K.; Foresman, J. B.; Ortiz, J. V.; Cui, Q.; Baboul, A. G.; Clifford, S.; Cioslowski, J.; Stefanov, B. B.; Liu, G.; Liashenko, A.; Piskorz, P.; Komaromi, I.; Martin, R. L.; Fox, D. J.; Keith, T.; Al-Laham, M. A.; Peng, C. Y.; Nanayakkara, A.; Challacombe, M.; Gill, P. M. W.; Johnson, B.; Chen, W.; Wong, M. W.; Gonzalez, C.; Pople, J. A. *Gaussian 03*, revision A.1; Gaussian, Inc.: Pittsburgh, PA, 2003.

(13) In the doublet electronic ground state $X^2\Pi_g$ of O_2^-, the bond length $r(O-O) = 1.3461$ [1.3620] Å for the B3LYP/A [QCISD/B] computational level, which agrees with the experimental value of 1.347 Å;[14a] B3LYP/B $r(O-O) = 1.351$ Å,[14b] MP2/6-311++G(3d,3p)+diffs(2s2p,s) $r(O-O) = 1.357$ Å,[6e] QCISD/aug-cc-pVTZ $r(O-O) = 1.3418$ Å,[14c] CCSD(T)/aug-cc-pVTZ $r(O-O) = 1.3563$ Å, and QCISD(T)/aug-cc-pVTZ $r(O-O) = 1.3574$ Å.[14c] Its stretching vibrational mode is predicted at 1165 (UB3LYP/A) and 1142 (UQCISD/B) cm^{-1} (cf. 1090 cm^{-1},[14b] and 1170.6 cm^{-1} (QCISD/aug-cc-pVTZ[14c]), 1103.5 cm^{-1} (CCSD(T)/aug-cc-pVTZ[14c]), 1107.8 cm^{-1} (QCISD(T)/aug-cc-pVTZ[14c])). The electronic energy amounts to −150.39171 [−149.96765] hartrees and ZPVE to 1.67 [1.63] kcal/mol. The water molecule is characterized by the equilibrium bond length $r(O-H) = 0.962$ [0.962] Å, bond angle ∠HOH = 105.0° [105.5°], and the harmonic frequencies [IR activities] (see ref 15): $\nu_2 = 1604$ [1645] cm^{-1} [66 (69) km/mol], $\nu_1 = 3815$ [3875] cm^{-1} [9 (6) km/mol], and $\nu_3 = 3920$ [4005] cm^{-1} [57 (49)] referred to the B3LYP/A [QCISD/B] computational level(s). Its ground-state electronic energy is equal to −76.45853 [−76.24141] hartrees and the ZPVE = 13.35 [13.62] kcal/mol.

(14) (a) Huber, K. P.; Herzberg, G. *Molecular Spectra and Molecular Structure*: *Constants of Diatomic Molecules*; Van Nostrand: New York, 1979. (b) Knak Jensen, S. J.; Mátyus, P.; McAllister, M. A.; Csizmadia, I. G. *J. Phys. Chem. A* **2001**, *105*, 9029. (c) Chandrasekher, C. A.; Griffith, K. S.; Gellene, G. I. *Int. J. Quantum Chem.* **1996**, *58*, 29 and references therein.

(15) *The Hydrogen Bond. Recent Developments in Theory and Experiments*; Schuster, P., Zundel, G., Sandorfy, C., Eds.; North-Holland: Amsterdam, The Netherlands, 1976.

(16) Jeffrey, G. A. *An Introduction to Hydrogen Bonding*; Oxford University Press: Oxford, UK, 1997.

(17) Ayotte, P.; Weddle, G. H.; Kim, J.; Johnson, M. A. *Chem. Phys.* **1998**, *239*, 485.

(18) Let us consider e.g. $\mathbf{I}_3$. $\mathbf{1d}^2$ corresponds to the $O_1-H_5\cdots O_2$ and $O_1-H_6\cdots O_4$ hydrogen bonds. The former is ionic $\mathbf{1d}_i$ whereas the latter is of a water−water type, $\mathbf{1d}_w$. **2d** corresponds to $O_{10}-H_9\cdots O_2$ and **3d** to $O_4-H_8\cdots O_3$. **d** stands for the H-bond donor and **a** for H-bond acceptor.

(19) Obviously, some caution in a complete assignment of the $O_5H_{10}\cdot\cdot\cdot O_1$ to the class of weak, water−water-like hydrogen bonds[15,16] is necessary. It is definitely a moderate hydrogen bond[15,16] because its stretching mode is downshifted by about 400 cm^{-1}.